Phase Equilibria, Molecular Conformation, and Dynamics in Phosphatidylcholine/Phosphatidylethanolamine Bilayers†

A. Blume,‡ R. J. Wittebort,§ S. K. Das Gupta, and R. G. Griffin*

ABSTRACT: Solid-state ^{13}C and ^{2}H NMR experiments have been used to examine the phase equilibria and dynamic structure of binary mixtures of diplamitoylphosphatidylcholine (DPPC) and dipalmitoylphosphatidylethanolamine (DPPE). The experiments rely on changes in the ^{13}C and ^{2}H spectra of *sn*-2 ^{13}C=O labeled and ^{2}H chain and head group labeled lipids at phase boundaries. In particular, broad powder patterns are observed in the gel state, and these patterns narrow dramatically in the liquid-crystalline phase. In the two-phase region a superposition of the gel-phase and liquid-crystalline-phase spectra is observed, which results from the presence of large domains in the DPPC/DPPE system. The appearance of the liquid-crystalline component and the disappearance of the gel component permit the solidus and liquidus curves of the phase diagram to be located accurately. Furthermore, a comparison of the temperature dependence of the ^{13}C and ^{2}H spectra shows the phase transition mechanism to be a function of composition. This result, together with other evidence, supports the hypothesis that the gel-state lattice changes from the $L_{\beta'}$ or $P_{\beta'}$ to the L_{β} configuration with increasing DPPE content. Finally, a detailed examination of the composition dependence of the spectra provides evidence for nonideal mixing.

Biological membranes are composed of lipids belonging to a variety of different classes. Of these, phosphatidylcholines (PC)[1] and phosphatidylethanolamines (PE) are two of the major components of most eukaryotic cells (Rouser et al., 1968), and consequently binary mixture of these two phospholipids are used as simple model systems to elucidate the phase behavior of biological membranes. In the past a variety of different physiochemical methods have been employed to investigate PC/PE mixtures; for example, ESR (Shimshick & McConnell, 1973; Luna & McConnell, 1978), fluorescence (Lu, 1976; Sklar et al., 1977), Raman (Mendelsohn & Taraschi, 1978; Mendelsohn & Koch, 1980), and ^{31}P NMR spectroscopies (Arnold et al., 1981) have been used to construct partial or complete phase diagrams for these binary lipid mixtures.

Despite these relatively extensive investigations, there remain a number of uncertainties about the phase behavior and other properties of these simple lipid mixtures. For instance, the position of the solid → fluid plus solid-phase boundary, as determined by ESR and fluorescence spectroscopies, differs from that obtained from DSC experiments. Secondly, the presence of the P_{β} or $P_{\beta'}$ phase at high DPPC concentrations leads to additional complications in this region of the phase diagram, which have yet to be resolved. In addition, ESR, fluorescence, and DSC techniques—which have been the primary methods used to construct phase diagrams—do not yield information on the molecular properties of the various phases or on the manner in which these properties change at phase boundaries. Thus, it is not known if there are changes in molecular conformation at phase boundaries and, if so, what these changes involve. A related interesting question concerns the rate of exchange or lateral diffusion between fluid and solid domains in the two-phase region of the phase diagram. In particular, is this exchange in DPPC/DPPE mixtures fast or slow compared to that observed in other binary lipid systems, for example, those containing cholesterol.

With these and other questions in mind, we have performed a ^{13}C and ^{2}H NMR investigation of DPPC/DPPE mixtures. In this work we have employed synthetically labeled lipids. Specifically, ^{13}C was introduced at the *sn*-2 C=O to produce 2[1-^{13}C]DPPC and 2[1-^{13}C]DPPE, and ^{2}H was placed at the 4 position of the *sn*-2 chain to yield 2[4,4-$^{2}H_2$]DPPC and 2[4,4-$^{2}H_2$]DPPE. The former compounds permit us to monitor the molecular conformation in the lipid glycerol backbone region, whereas the latter permit study of the acyl chain region. In addition, we have employed head group labeled DPPE to study the structure and dynamics of the head group region. The results of these investigations indicate that these NMR techniques can provide valuable insights into the molecular dynamics and conformation of these systems. For example, the ^{13}C spectra are particularly sensitive to the formation of liquid-crystalline lipid molecules and permit the location of phase boundaries with great accuracy. Furthermore, domains in the two-phase region of the phase diagram are large, and the ^{2}H chain spectra and the ^{13}C spectra clearly show a superposition of gel and liquid-crystalline line shapes. The spectra also indicate that the phase transition mechanism in the DPPC/DPPE system varies with composition, and, finally, they permit an examination of the deviation from ideal miscibility in the gel and liquid-crystalline phases.

Materials and Methods

[1-^{13}C]Palmitic acid was purchased from Kor Isotopes (Cambridge, MA). The synthesis of ^{2}H-labeled fatty acids is described elsewhere (Das Gupta et al., 1982). 2[1-^{13}C]-DPPC and 2[4,4-$^{2}H_2$]DPPC were prepared by acylation of the corresponding lysophosphatidylcholine according to the

† From the Francis Bitter National Magnet Laboratory, Massachusetts Institute of Technology, Cambridge, Massachusetts 02139. *Received February 25, 1982; revised manuscript received July 8, 1982.* This research was supported by the National Institutes of Health (GM-23289, GM-25505, and RR-00995) and by the National Science Foundation through its support of the Francis Bitter National Magnet Laboratory (C-670). A.B. was supported by a research scholarship from the Deutsche Forschungemeinschaft (B1 182/2-4) and R.J.W. by a U.S. Public Health Service postdoctoral fellowship (GM-07215).

‡ Present address: Institut für physikalische Chemie II, D-7800 Freiburg, Federal Republic of Germany.

§ Present address: Department of Chemistry, University of Louisville, Louisville, KY 60292.

[1] Abbreviations: DPPC, dipalmitoylphosphatidylcholine; DMPC, dimyristoylphosphatidylcholine; DPPE, dipalmitoylphosphatidylethanolamine; DMPE, dimyristoylphosphatidylethanolamine; T_{onset}, temperature of onset of melting; T_{comp}, temperature of completion of melting; ESR, electron spin resonance; NMR, nuclear magnetic resonance; DSC, differential scanning calorimetry; TLC, thin-layer chromatography; Tempo, 2,2,6,6-tetramethylpiperidinyl-1-oxy.

0006-2960/82/0421-6243$01.25/0

method of Gupta et al. (1977). 2[1-^{13}C]DPPE and 2[4,4-$^{2}H_2$]DPPE were synthesized similarly by reacylating *N*-(*tert*-butyloxycarbonyl)lysophosphatidylethanolamine (Chakrabarti & Khorana, 1975). Ethanolamine-*1*-d_2 was prepared by reduction of glycine ethyl ester with $LiAlD_4$ (Weissbach & Sprinson, 1953). Head group labeled DPPE was synthesized according to the procedure of Eibl (1978). 1,2-Dipalmitoyl-*sn*-glycerol was converted to 1,2-dipalmitoyl-*sn*-glycero-3-phosphoric acid dichloride by phosphorylation with phosphorous oxychloride and coupled to ethanolamine-*1*-d_2 in the presence of triethylamine.

Samples for NMR consisted of ~50 mg of deuterated or ^{13}C-labeled lipid mixed with the appropriate amount of unlabeled lipid dispersed in an equal amount of H_2O [^{2}H-depleted H_2O (Aldrich Chemicals, Milwaukee, WI) in the case of ^{2}H NMR experiments]. Mixing was achieved by dissolving the phospholipids in $CHCl_3$ and then evaporating the solvent at high temperature in a stream of nitrogen. The lipid mixtures were then dried for 24 h under high vacuum to remove residual $CHCl_3$. The lipids were sealed in 7-mm glass tubes. The purity of the samples was checked by TLC before and after the experiments. The pH of the dispersions was adjusted to 7 in order to avoid decomposition.

NMR Spectroscopy. ^{13}C and ^{2}H spectra were obtained on a home-built pulse spectrometer operating at 73.9 MHz for ^{13}C and 45.1 MHz for ^{2}H (294 MHz for ^{1}H). High-temperature ^{13}C spectra of lipids in the liquid-crystalline phase were recorded with a simple Hahn spin-echo. Gel-state spectra were generally recorded with standard cross-polarization (Pines et al., 1973), together with a 180° refocusing pulse at the ^{13}C frequency to circumvent receiver overload (Griffin, 1981). Because the spectral effects are strongly temperature dependent, care has to be taken to avoid sample heating by the strong ^{1}H-decoupling fields. ^{1}H-decoupling power was therefore kept at the minimum level necessary to obtain well-resolved lines. In addition, recycle delays of typically 5 s were used to minimize radio-frequency heating. The ^{13}C $\pi/2$ pulse was ~3 μs. About 500–5000 echos were accumulated, depending on the sample temperature and the amount of labeled lipid in the sample. All shifts are referenced to external benzene. ^{2}H NMR spectra were recorded with a two-pulse quadrupole echo sequence (Solomon, 1958; Davis et al., 1976) using a $\pi/2$ pulse of ~1.7 μs and a pulse separation of 40 μs. Dwell times for low-temperature gel-phase spectra were generally 0.2 or 0.5 μs and for liquid-crystalline spectra 2 μs. From 5000 to 40000 echos were accumulated with a recycle delay of 0.2 s, depending on the type of spectrum and the amount of lipid in the sample. Phase cycling as well as quadrature detection was used in both cases (Griffin, 1981).

^{2}H NMR absolute intensity spectra were obtained by dividing the time-domain signal by the number of scans and multiplying by a constant factor as described before (Blume et al., 1982). This requires that the spectrometer sensitivity remain constant over the temperature range studied, as discussed previously (Blume et al., 1982).

Results

Shown in Figures 1 and 2 are ^{13}C spectra of 1:1 and 1:3 DPPC/DPPE mixtures, those in the left column being for 2[1-^{13}C]DPPC/DPPE and those in the right column for DPPC/2[1-^{13}C]DPPE.[2] The signals on the right side of each spectrum, between 20 and 160 ppm, arise from natural abundance ^{13}C nuclei of the acyl chains, the head group, and

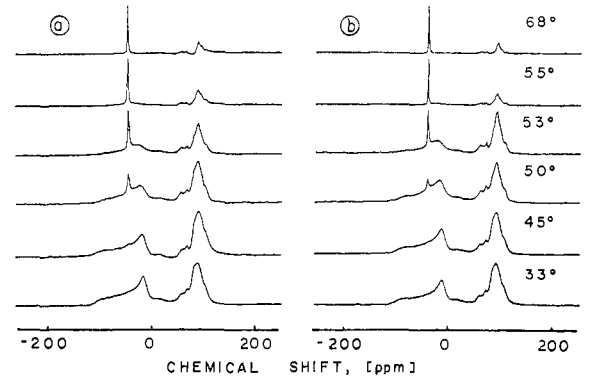

FIGURE 1: Proton-decoupled ^{13}C NMR spectra of 1:1 mixtures of (a) 2[1-^{13}C]DPPC/DPPE and (b) DPPC/2[1-^{13}C]DPPE in 50 wt % H_2O as a function of temperature.

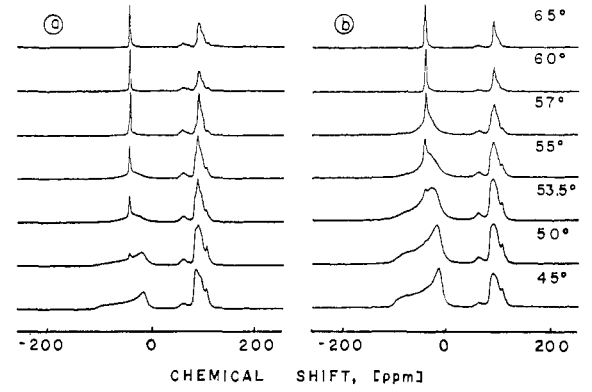

FIGURE 2: Proton-decoupled ^{13}C NMR spectra of 1:3 mixtures of (a) 2[1-^{13}C]DPPC/DPPE and (b) DPPC/2[1-^{13}C]DPPE in 50 wt % H_2O as a function of temperature.

the glycerol backbone region. The prominent pattern on the left side of the spectra is the signal from the labeled carbonyl group of the *sn*-2 chain of the lipid. At temperatures below the phase transition region of the mixtures, the powder pattern is axially symmetric with a temperature-dependent width that varies from 95 to 105 ppm. This line shape is characteristic of lipid molecules undergoing fast (on the ^{13}C time scale) axial diffusion about the long axis of the molecule. It has been observed previously for 2[1-^{13}C]DPPC in the $L_{\beta'}$ phase (Wittebort et al., 1981, 1982) and 2[1-^{13}C]DPPE in the L_β phase (Blume et al., 1982). The width of this powder pattern is determined by the rigid lattice tensor, which is slightly asymmetric (σ_{11} = −132 ppm, σ_{22} = −12 ppm, and σ_{33} = 11 ppm for 2[1-^{13}C]DPPE), and by the orientation of the tensor relative to the diffusion axis. Above the phase transition region, the broad powder patterns collapse to isotropic-like lines characteristic of the L_α phase. The formation of the L_α phase leads to a conformational change in the backbone region of the molecule that fortuitously tilts the *sn*-2 carbonyl tensor to the "magic angle", resulting in an isotropic-like line (Wittebort et al., 1982).

Inside the transition region of the mixture "solid" and "fluid" phases should coexist, and the fluid phase should be enriched with the lower melting component. Inspection of Figures 1 and 2 shows that this is indeed the case for temperature between 45 and 55 °C for the 1:1 DPPC/DPPE mixture and between 50 and 60 °C for the 1:3 DPPC/DPPE mixture. In all cases a superposition of the L_β powder pattern and L_α line is observed inside the transition region, and the L_α line in the mixtures with 2[1-^{13}C]DPPC has a larger intensity than in the respective mixture containing 2[1-^{13}C]DPPE. This can clearly be seen, for instance, in parts a and b of Figure 1 by

[2] In referring to DPPC/DPPE mixtures, we use the convention that the first number in the ratio refers to DPPC and the second to DPPE. Thus, 1:3 indicates a 25 mol % DPPC/75 mol % DPPE mixture.

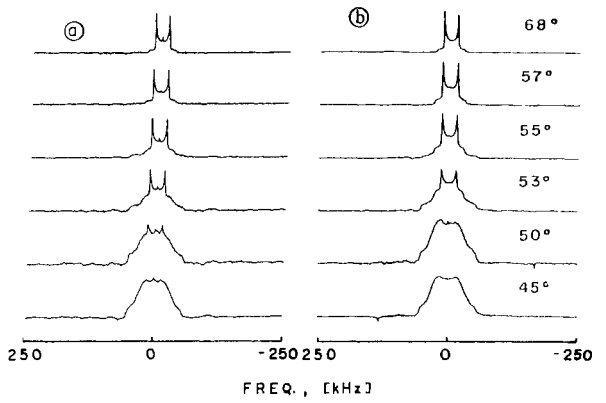

FIGURE 3: ^2H NMR spectra of 1:1 mixtures of (a) 2[4,4-$^2H_2$]-DPPC/DPPE and (b) DPPC/2[4,4-$^2H_2$]DPPE in 50 wt % deuterium-depleted H_2O as a function of temperature.

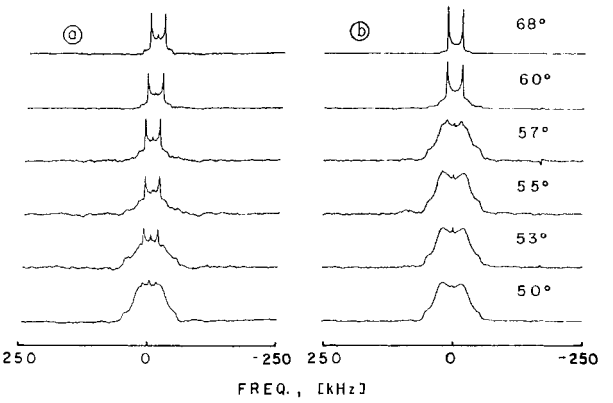

FIGURE 4: ^2H NMR spectra of 1:3 mixtures of (a) 2[4,4-$^2H_2$]-DPPC/DPPE and (b) DPPC/2[4,4-$^2H_2$]DPPE in 50 wt % deuterium-depleted H_2O as a function of temperature.

comparing the spectra taken at 50 or 53 °C, respectively. (The signals from the natural abundance ^{13}C nuclei are much larger in Figure 2a, of course, because only 25% of the total lipids are labeled as compared to 75% for the case where the DPPE is labeled.)

It should be noted that in all instances the spectra are not simple superpositions of L_β powder patterns and L_α lines. The L_α lines are generally wider than those in the pure L_α phase, and the line shapes for the L_β pattern change when the fraction of the L_α line increases. These effects are due to exchange between two components. One would expect that the exchange rates between liquid-crystalline- and gel-state domains depend on several factors, i.e., the proportion of a liquid-like lipid, the size of the gel-state and liquid-crystalline-state domains, and the absolute temperature. Moreover, because the lipid molecules have to diffuse laterally from solid to liquid domains, the temperature dependence of the diffusion coefficients within a domain has to be taken into account. All these factors should lead to an increase in the exchange rates with increasing temperature, and thus to exchange broadening of the lines in the transition region. This is indeed observed and is easily discerned in the 55 and 57 °C spectra of Figure 2b, which have markedly different line shapes than, for instance, the spectra taken at 50 and 53 °C in Figure 1a.

From spectra like those shown in Figures 1 and 2 it is possible to determine the phase boundaries for the two-phase region in the DPPC/DPPE phase diagram. The solidus line is determined from the spectra of the lower melting component, 2[1-^{13}C]DPPC, by observing the first appearance of the L_α-like line superimposed on the gel-state powder pattern. Similarly, the position of the liquidus curve, associated with the completion of melting, is obtained from the 2[1-^{13}C]DPPE spectra by observing the disappearance of the powder pattern. The temperatures for the onset and completion of melting determined by this method are shown in Figure 7. Included are data points from mixtures containing 15, 25, and 33% DPPE (spectra are not shown). In principle it should also be possible to determine the tie lines in the phase diagram from the relative intensities of the L_α and L_β patterns. However, there are certain limitations to a quantitative evaluation of the tie lines, and these will be discussed below.

To observe changes in the acyl chain region of the lipids, we investigated mixtures of DPPC and DPPE where one of the lipids is specifically ^2H labeled at the 4 position of the 2 chain. In Figures 3 and 4 are shown spectra of 1:1 and 1:3 mixtures of DPPC with DPPE where either DPPC (left) or DPPE (right) is labeled. At temperatures below the phase transition (i.e., 25 °C) the spectral line shapes are characteristic of molecules executing long-axis rotation with rotational jump rates of (3–4) $\times 10^5$ s^{-1}. In this respect, the spectra are not markedly different from those observed for pure DPPE in the gel state (Blume et al., 1982). Above the phase transition region the characteristic sharp powder pattern with $\Delta\nu_{Q\perp} \simeq 30$ kHz is seen, indicating liquid-crystalline lipid molecules undergoing fast rotational diffusion and gauche–trans isomerization. In the phase transition region a superposition of gel-state and liquid-crystalline-state powder patterns is observed. Like in the ^{13}C spectra, the lower melting component (DPPC) is more sensitive to the onset of melting, and the intensity of the L_α pattern at any temperature inside the phase transition region is larger for DPPC because the liquid-crystalline phase is enriched with DPPC. The ^2H spectra in the phase transition region also manifest the effects of exchange in two ways. First, the line shapes are broadened, and secondly, the overall intensity of the spectrum is decreased. The latter effect is due to quadrupole echo distortions and occurs when the correlation times for the motions are comparable to the reciprocal of the rigid lattice quadrupole coupling. In this case T_2 is anisotropic, and for certain regions of the powder pattern, it becomes comparable to the τ value in the echo sequence. Magnetization from these regions is not refocussed, and distorted spectra with decreased spectral intensities are observed (Spiess & Sillescu, 1981). The effect is illustrated in Figure 5, where we have plotted spectra of a 1:3 DPPC:2-[4,4-$^2H_2$]DPPE mixture on an absolute intensity scale. The intensity of the 1 °C spectrum is depressed since the (intramolecular) axial diffusion rate is the intermediate exchange regime ($R_R \simeq 2.1 \times 10^5$ s). The central portions of the line shape—e.g., the perpendicular edges—are most strongly modulated, and thus affected, by this motion. With increasing temperature the intensity increases until temperatures of about 55 °C are reached, where a second decrease in spectral intensity is observed. Again, this indicates the presence of a motional process with a correlation time of 10^{-4}–10^{-5} s. From Figure 5 it is evident that the axial diffusion rates of the gel fraction are approaching fast-limit conditions and similar behavior would be expected from any liquid-crystalline fraction at these temperatures. Thus, we believe the decrease in echo intensity observed at 57 °C arises from intermediate rate exchange between gel and liquid-crystalline domains.

Finally, we have studied the head group region in DPPC/DPPE mixtures, and Figure 6 shows typical spectra of $^+NH_3$–CH_2–CD_2–DPPE in a 3:1 mixture. In accordance with previous findings of Seelig & Gally (1976) a residual quadrupole splitting of ca. 10 kHz is observed for DPPE in the liquid-crystalline state. Below the phase transition region

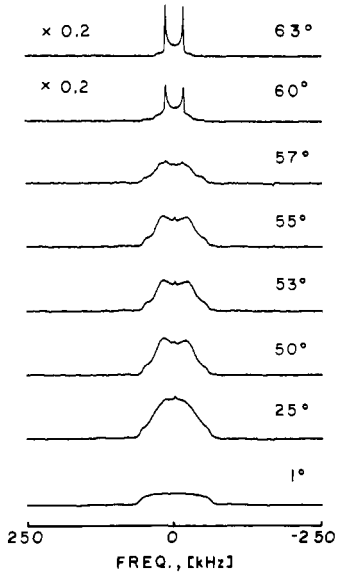

FIGURE 5: ^2H NMR spectra of a 1:3 mixture of DPPC/2[4,4-$^2H_2$]DPPE as a function of temperature. The spectra are scaled according to the absolute intensity of the quadrupole echo. The spectrum at 1 °C shows low intensity due to intermediate rotational rate. The decrease of spectral intensity in the 55 and 57 °C spectra is due to intermediate exchange between liquid and solid lipids.

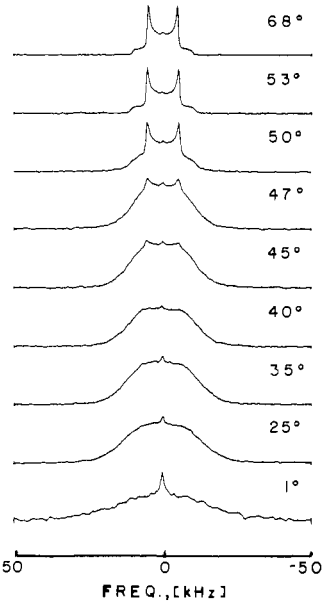

FIGURE 6: ^2H NMR spectra of a 3:1 mixture of DPPC with $^+NH_3$–CH_2–CD_2–DPPE in 50 wt % deuterium-depleted water as a function of temperature.

head group labeled DPPE gives a wide featureless line of ca. 16-kHz width. This has been interpreted previously as being caused by slow conformational changes within the head group superimposed on faster axial rotational diffusion of the whole molecule (Blume et al., 1982). At low temperatures (1 °C) the effect of the decrease of the axial rotation rates can clearly be seen. The echo intensities decrease drastically, leading to lower S/N ratios. (The spectra in Figure 6 are are not plotted on an absolute intensity scale.) Note that inside the phase transition region spectra corresponding to liquid and solid DPPE molecules can clearly be discerned.

Discussion

The information most readily available from ^{13}C as well as ^2H NMR spectra of lipid mixtures are the temperatures of onset and completion of melting, which correspond to points

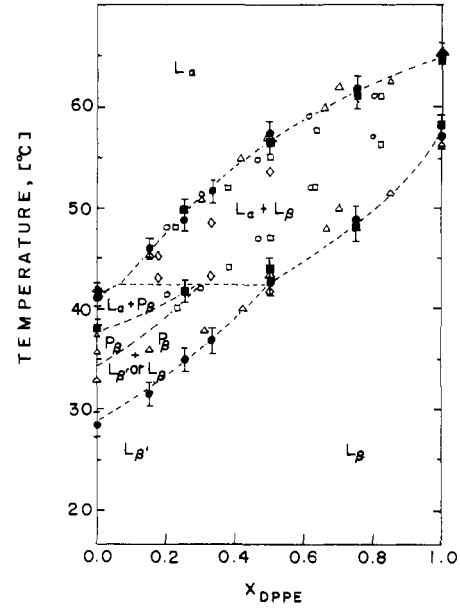

FIGURE 7: Experimental temperature vs. composition diagram for aqueous dispersions of DPPC/DPPE mixtures: (●) data from ^{13}C NMR; (■) data from ^2H NMR. Included are data obtained with other physical techniques: (○) Tempo spin-label (Shimshick & McConnell, 1973); (△) calorimetry (Blume & Ackermann, 1974); (□) chlorophyll a fluorescence (Lee, 1976); (◇) Raman spectroscopy (Mendelsohn & Koch, 1980).

on the solidus and liquidus curve, respectively, in a binary phase diagram. The sensitivity of the ^{13}C spectra to the appearance of an L_α-like line, particularly when the lower melting component is monitored, has been mentioned before. In addition ^2H NMR spectra of chain-labeled lipids are suitable for this purpose, but the positions of the phase boundaries are probably less accurate. The reasons for this are primarily that the two transitions of the $I = 1$ powder pattern overlap and, at the same time, the difference between the gel and liquid-crystalline spectral breadths amounts to only a factor of 2. In the ^{13}C spectra the difference in spectral widths is about 10^2. In addition, echo distortions arising from slow-exchange processes can lead to spectral distortions, and the ^{13}C experiment does not suffer from this problem. Nevertheless, for reasons to be discussed below it is advantageous to investigate both types of spectra.

The proposed DPPC/DPPE phase diagram obtained from the ^{13}C and ^2H spectra is shown in Figure 7. Included are data obtained from various physical techniques, i.e., ESR spin-labels (Shimshick & McConnell, 1973), calorimetry (Blume & Ackermann, 1974), chlorophyll a fluorescence (Lee, 1976), and Raman spectroscopy (Mendelsohn & Koch, 1980). While the agreement between the data for the liquidus curve is generally satisfactory, the various methods apparently monitor quite different temperatures for the onset of melting. In particular, the probe methods like ESR spin-label and fluorescence spectroscopy report somewhat higher temperatures than do calorimetry and NMR. These discrepancies probably arise from inherent differences between probe methods and intrinsic methods like calorimetry and NMR.

In ESR experiments the distribution of the water-soluble spin-label Tempo between aqueous-phase and fluid-lipid regions is monitored via a spectral parameter f. A change in the slope of this parameter is generally taken as an indication for a phase boundary. In the case of lipid mixtures, calorimetric scans show that the transition regions are often very wide and asymmetric, with a slow increase of the heat capacity on the low-temperature side (Blume, 1980). Detection of the

deviation from the base line (indicating the onset of melting) of the calorimetric curve can be quite difficult, and the onset temperatures, therefore, have rather large errors. Correspondingly, the change in the spin-label spectral parameter takes place over a wide temperature range, and the exact determination of the onset of melting is difficult. The same argument holds for chlorophyll a fluorescence measurements where the fluorescence intensity is monitored. This intensity decreases with the formation of nonfluorescent, aggregated chlorophyll a molecules below the phase transition in the gel state. Both methods seem to be less sensitive than calorimetry and NMR when broad asymmetric transitions are encountered.

In the particular case of the DPPC/DPPE phase diagram an additional interesting complication arises from the presence of the intermediate $P_{\beta'}$ or P_{β} phase of pure DPPC (Janick et al., 1976, 1979; Stamatoff et al., 1982) in that part of the phase diagram where the DPPE concentration is low. The presence of this phase was neglected in earlier studies of DPPC/DPPE mixtures; however, it has recently been discussed in the determination of phase diagrams of phosphatidylcholine/phosphatidylserine and DMPC/DPPC mixtures (Luna & McConnell, 1977, 1978). The calorimetrically determined onset of melting temperatures in the left part of the phase diagram on Figure 7 include the pretransition, which is very broad and shows no distinct separation from the main transition. Similar results have been obtained for the related DMPC/DMPE phase diagram by Chapman et al. (1974), where it was observed that the separation between the pretransition and main transition regions disappears after the addition of 10% DMPE. ^{13}C NMR of carbonyl group labeled lipids has been shown before to be sensitive to the formation of the intermediate phase in pure DPPC (Wittebort et al., 1981). Thus, in the left part of the phase diagram of Figure 7 the "onset of melting" determined by ^{13}C NMR is in reality the onset of the formation of the $P_{\beta'}$ phase. The temperatures for the $P_{\beta'}$-phase formation determined by ^{13}C NMR are generally lower than those found by calorimetry. This is also true for pure DPPC (Wittebort et al., 1981, 1982) and has been verified again in the course of this study. Although we have no completely satisfactory explanation for this discrepancy, it is possibly due to kinetic effects (Lentz et al., 1978).

In contrast, ^2H NMR spectra of chain-labeled DPPC do not appear to be very sensitive to the formation of the $P_{\beta'}$ phase. This is illustrated in Figure 8 where we show ^{13}C and ^2H NMR spectra of DPPC. In the ^{13}C spectra on the left side the isotropic-like line can clearly be seen in the 32 °C spectrum. It increases in intensity with higher temperature and dominates the 38° spectrum. Although the spectra of 2[4,4-$^2H_2$]DPPC on the right side of Figure 8 do show what appears to be a superposition of different powder patterns in the $P_{\beta'}$ region, there is no well-resolved, sharp component with a reduced quadrupole splitting characteristic of the L_{α} phase visible up to ca. 39 °C, the beginning of the main transition. Similar behavior is observed for other lecithins—e.g., in the $P_{\beta'}$ phase of pure DMPC a sharp component is visible in the *sn*-2 $^{13}C{=}O$ spectra but not in ^2H spectra of chain-labeled DMPC. This observation suggests that on a molecular level the conformational change at the *sn*-2 $^{13}C{=}O$ precedes melting of the acyl chains, and as discussed elsewhere, this conformational change may be due to a locally varying tilt present in the $P_{\beta'}$-rippled structure (Wittebort et al., 1982). This phenomenon is not restricted to pure PC's but occurs even in the presence of 25% DPPE as is illustrated in Figure 7. The isotropic-like line in the ^{13}C spectrum appears at 35 °C, indicating the transition

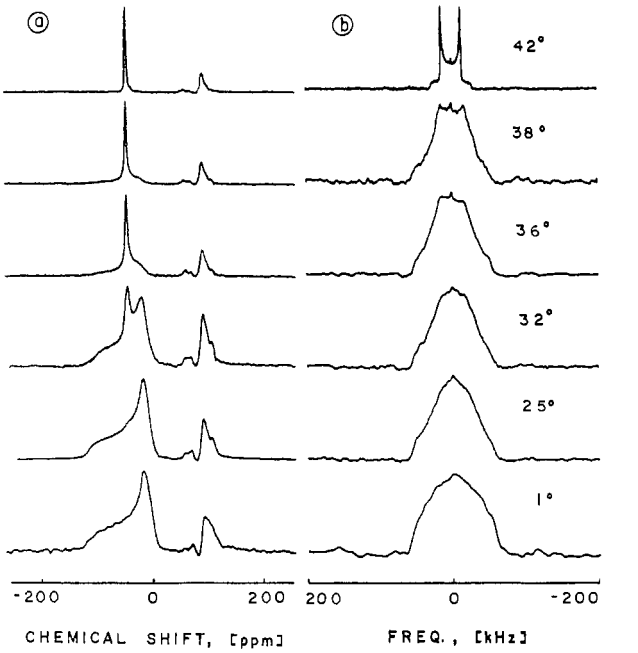

FIGURE 8: (a) Proton-decoupled ^{13}C NMR spectra of 2[1-^{13}C]DPPC in 50 wt % H_2O as a function of temperature. (b) ^2H NMR spectra of 2[4,4-$^2H_2$]DPPC in 50 wt % H_2O as a function of temperature.

to a P_{β} or $P_{\beta'}$ phase, whereas true chain melting is not observed until the temperature reaches 42 °C as indicated by the appearance of the sharp powder pattern in the ^2H NMR spectrum. However, a quite different behavior is seen at higher DPPE levels, for example, in 1:1 DPPC/DPPE mixtures and in pure DPPE (Blume et al., 1982). In both of these latter cases sharp liquid-crystalline lines appear simultaneously in the ^{13}C and the ^2H spectra (see Figures 1 and 3). This result emphasizes the fact that the phase transition mechanism can change dramatically with varying composition, a possibility of which we were aware before we began these investigations. It is partially for this reason that we have studied both ^{13}C and ^2H spectra of both lipids in the mixture.

We have mentioned before that in principle it should be possible to determine the tie lines in the phase diagram from the ^{13}C spectra in the phase transition region. Specifically, if the fractions of both lipids in the fluid state are known, then we can calculate X_B^l and X_B^s, the equilibrium compositions of the liquid and solid phases, according to the standard expressions:

$$X_B^l = \frac{f_B^l X_B}{f_B^l X_B + f_A^l (1 - X_B)} \quad (1)$$

$$X_B^s = \frac{f_B^s X_B}{f_B^s X_B + f_A^s (1 - X_B)} \quad (2)$$

where X_B is the mole fraction of component B in the total mixture, f_A^l and f_B^l are the fractions of liquid, and f_A^s and f_B^s are the fractions of solid components A and B, respectively. These data then correspond to points on the liquidus and solidus curve, respectively. The fractions f_A^l and f_B^l have to be determined from the line shapes of the ^{13}C carbonyl resonance. These lines, however, are not simple superpositions of L_{α}-like lines and L_{β} powder patterns due to exchange of molecules between two phases.

In Figure 9 we show computer simulations of the line shapes expected when both components are present in equal amounts and the exchange rate is varied. The particular model we used is that of a six-site chemical exchange, the details of which

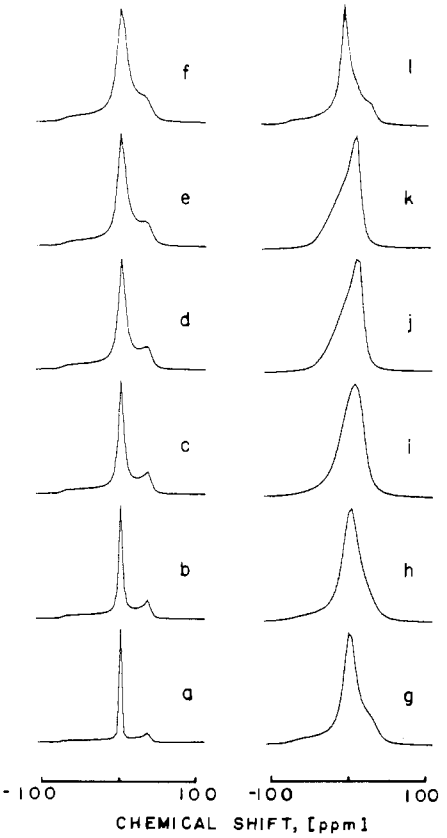

FIGURE 9: Computer simulations of ^{13}C spectra in the two-phase region. The model consists of an axially symmetric ^{13}C tensor of 143-ppm width executing three-site rotational jumps with a rate $R_R = 1 \times 10^6$ s^{-1}. An orientation of 27° with respect to the rotation axis leads to an axially reduced pattern of ~95-ppm width. Orientation at the magic angle (54.7°) gives an isotropic-like line. Different exchange rates R_{ex} between the two orientations affect the line shape. The probabilities for both sites were taken as 0.5. R_{ex} values are (a) 0, (b) 1×10^2 s^{-1}, (c) 2×10^2 s^{-1}, (d) 3×10^2 s^{-1}, (e) 4×10^2 s^{-1}, (f) 5×10^2 s^{-1}, (g) 7×10^2 s^{-1}, (h) 1×10^3 s^{-1}, (i) 2×10^3 s^{-1}, (j) 3×10^3 s^{-1}, (k) 5×10^2 s^{-1}, and (l) superposition of spectra (b–k) scaled according to the root mean square displacement as described in the text.

will be described in a separate publication (R. J. Wittebort and R. G. Griffin, unpublished results). We assume two types of molecules, both are allowed to execute rapid (1×10^6 s^{-1}) 3-fold (120°) jumps about the long axis. One type produces an L_β spectrum, accomplished by orienting an axially symmetric rigid lattice tensor (in this case of 10.58-kHz width) at an angle of 27° with respect to the rotation axis, while the other type gives a single ca. 150 Hz wide line (tensor axis tilted at the magic angle). Figure 9 shows the effect of increasing exchange rates on the line shape ($f^l = f^s = 0.5$). In the slow-exchange regions ($R_{ex} < 2 \times 10^2$ s^{-1}) the spectra clearly show the superposition of the L_α line and the L_β powder pattern, while increased exchange rates broaden the L_α line. In the fast-exchange regions ($R_{ex} > 4 \times 10^3$ s^{-1}) the original L_β powder pattern has disappeared, and the line shape resembles an axially symmetric pattern of reduced breadth. Inspection of the spectra in Figures 1 and 2 shows that the simulations resemble qualitatively the experimental spectra in the phase transition region, particularly at lower temperatures, i.e., in mixtures with 50% DPPE. However, the line shapes cannot be simulated quantitatively with this simple model. Note that the underlying L_β powder pattern in the spectra of Figure 1 at 50 and 53 °C becomes more rounded with higher temperature. In the simulations this can be achieved by increasing the exchange rate R_{ex} to 5×10^2 s^{-1}. However, the broadening also affects the L_α line as well (see Figure 9), while in the experimental spectra this line stays fairly sharp and increases only slightly in width. Thus a better fit cannot be achieved by simply increasing R_{ex}. Even more evident are the discrepancies between simulations and experimental spectra at higher temperatures, i.e., for 1:3 DPPC/DPPE mixtures (see Figure 2). The effect that the L_β powder pattern is strongly distorted, while the L_α line is very sharp, is especially evident in the 55 and 57 °C spectra of Figure 2b. The simple model we have used in the simulations, two lipid components and only one exchange rate, cannot reproduce these experimental line shapes. It should be emphasized that in other cases, i.e., pure PC, PC/cholesterol and PE/cholesterol mixtures, this model is applicable and yields quite good simulations of the experimental spectra (Wittebort et al., 1982; Blume & Griffin, 1982).

An improved fit of the simulations can be obtained in different ways. One possibility would be to include a third component corresponding to lipids in the boundary regions between different domains. Those lipids could have some intermediate behavior, i.e., the carbonyl tensor axis could be oriented at a different angle with respect to the rotation axis. Difficulties arise, however, from the unknown amount of boundary liquids, their spectral behavior, and the necessity to introduce two possibly different exchange rates, one for the exchange of boundary lipid with gel-state lipid, the other for exchange with liquid-crystalline lipid. Another way would be to introduce a distribution of exchange rates, and the following considerations will illustrate the rationale for this proposition.

The observed exchange between the L_α and L_β lines is due to translational diffusion of lipid molecules from liquid-crystalline domains to gel-state domains and vice versa. The exchange rate is thus governed by the diffusion coefficients of the lipid molecules in both phases. The coefficients for translational diffusion in the liquid-crystalline phase were generally found to be ca. 1×10^{-8} cm^2 s^{-1} to 2×10^{-7} cm^2 s^{-1} for saturated phosphatidylcholines, depending on the method used (Devaux & McConnell, 1972; Sackmann & Träuble, 1972; Wu et al., 1977; Naqvi et al., 1974; Galla et al., 1979; Rubinstein et al., 1979), while the diffusion coefficients in the gel phase are about 2 orders of magnitude lower. For instance, Rubinstein et al. (1979) report a value of 7×10^{-11} cm^2 s^{-1} for DMPC at 16 °C. No data exist for pure PE or PC/PE mixtures, so for our purposes we assume that the diffusion coefficients in these systems are at least of the same order of magnitude. The mean square displacement $\bar{x}^2$ of a molecule diffusing in two dimensions is proportional to the diffusion coefficient D_T and t, the time:

$$\bar{x}^2 = 4D_T t \qquad (3)$$

In the ^{13}C NMR experiments the line shapes are sensitive to changes in exchange rates between 1×10^{-2} and 2×10^{-4} s. Taking for instance a lifetime of 2×10^{-3} s, which corresponds to intermediate exchange rates on the ^{13}C time scale (see Figure 9), and a D_T value of 1×10^{-10} cm^2 s^{-1}, we find for $\bar{x}^2$ a value of 8×10^{-13} cm^{-2} or 8×10^3 Å^2. In a recent report by Hui (1981), liquidus and solidus domains in the phase transition region of a lipid mixture were visualized for the first time with electron diffraction. The average width of the domains was reported to be between 0.2 and 0.5 μm, and assuming a circular domain, one would calculate domain areas of 3×10^6 to 7×10^7 Å^2. Thus, the domain sizes in the two-phase region are much larger than the mean square displacement reported on the intermediate exchange time scale of the ^{13}C experiments. In other words, a considerable fraction of the molecules, i.e., those in the middle of a particular domain

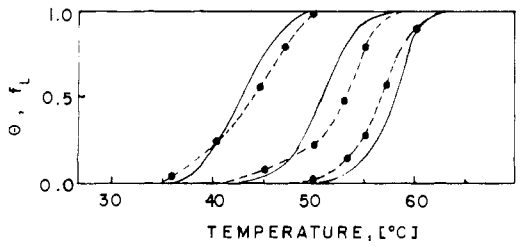

FIGURE 10: Degree of transition θ (—) calculated from calorimetric curves (Blume, 1976) and fraction of liquid-crystalline lipid f_L (--) estimated from ^{13}C spectra for 3:1 (left), 1:1 (middle), and 1:3 (right) DPPC/DPPE mixtures.

at a given time, are not able to reach the domain boundary in the characteristic time of the ^{13}C NMR experiment. Therefore, these molecules are reported as either solid or liquid lipid, while those immediately next to the domain boundary possibly belong to a class of fast-exchanging lipids.

The obvious extension of this model is to include intermediate exchange rates and to scale the exchange rate distribution function according to eq 3, i.e., to the distance from the domain boundary. A spectrum simulated according to this model is shown in Figure 9l. It was generated from a superposition of spectra b–k in Figure 9, where each spectrum was multiplied by the appropriate scaling factor. This line shape is different from the other simulated spectra in that it shows a sharper L_α-like line and a rounded L_β pattern, two features which are observed in the 57 °C spectrum in Figure 2b. This example shows that a qualitatively better fit can be obtained with these considerations. However, an attempt to simulate all spectra in the transition region by this approach does not seem sensible at the present time for a number of reasons. For example, the applied distribution function is rather arbitrary, the domain sizes and shapes in this particular system are not known, and the diffusion coefficients can only be estimated. In addition, a distribution of domain sizes and temperature-induced changes of all these parameters should be included. Thus, the number of unknown variables is large, and it is not possible to obtain a unique fit of the line shapes.

Nevertheless, it is still possible to obtain some semiquantitative information from the ^{13}C spectra. In particular, we have compared the experimental spectra with an extensive set of computer-simulated line shapes generated by using different exchange rates and different fractions from the L_α line. The height of the L_α line was the main criterion used for the amount of L_α lipid present in the mixture. Figure 10 shows plots of f_L, the total amount of liquid lipid, determined by ^{13}C NMR with this method. For comparison, normalized DSC transition curves, obtained by integration of the calorimetric scans, are also depicted (Blume & Ackermann, 1974; Blume, 1980). While the agreement between the temperatures of the onset of melting and those of the completion of melting is generally satisfactory, there are obvious deviations in the middle parts of the transition curves. Correspondingly, the equilibrium concentrations X_A^l and X_A^s determined from the f values according to (1) and (2) show noticeable deviations from the phase boundaries determined by the appearance and disappearance of the L_α and L_β lines, respectively. Specifically, the calculated data points all lie inside the two-phase region of the phase diagram. These deviations can be explained by the considerations discussed in relation to Figure 9. At the same time this crude method for the determination of the L_α fractions does reproduce the shapes of the transition curves fairly well. Moreover, the agreement between the melting onset and completion temperatures lends credibility to the method we have employed to determine the positions of the liquidus and solidus lines. Finally, it should be mentioned that

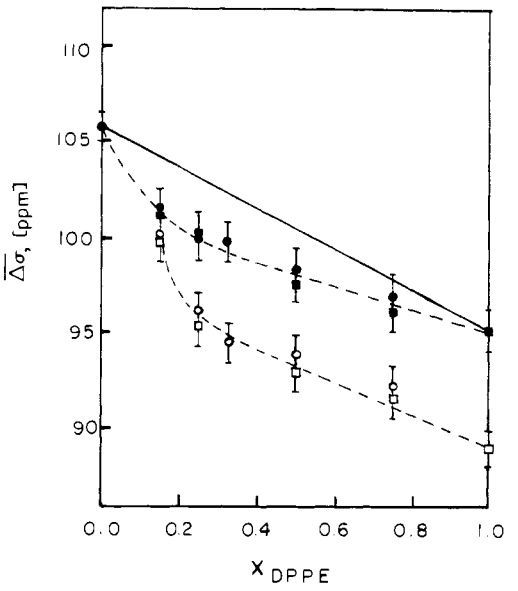

FIGURE 11: Residual chemical shift anisotropy of the *sn*-2 $^{13}C{=}O$ powder patterns in DPPC/DPPE mixtures: (●) 2[1-^{13}C]DPPC at 25 °C; (○) 2[1-^{13}C]DPPC at $T = T_{onset}$; (■) 2[1-^{13}C]DPPE at 25 °C; (□) 2[1-^{13}C] DPPE at $T = T_{onset}$.

the transition curves of Figure 10 show better agreement than do corresponding data for DPPE/CHOL mixtures. In the latter case the transitions are apparently of lower cooperativity (Blume & Griffin, 1982).

The ^2H NMR spectra of Figures 3, 4, and 6 should contain the same type of information about the L_α fraction as the ^{13}C spectra, and a decomposition of spectra in the phase transition region should theoretically be possible. However, in addition to the difficulties in the simulations described for the ^{13}C spectra, we encounter drastic decreases in the signal-to-noise ratio in the transition region due to exchange effects, which decrease the solid echo amplitude. Moreover, the folding of the transitions in the $I = 1$ ^2H spectra leads to an additional loss of resolution. Therefore, a determination of liquid fractions by ^2H NMR was not attempted.

Another of the primary goals of the ^{13}C and ^2H NMR experiments reported here was to examine the molecular conformation and dynamics of DPPC and DPPE in the various phases of a lipid mixture. As discussed above, the temperature dependence of the spectra of Figures 1–4 and 6 indicate substantial changes in these properties at phase boundaries. Other more subtle changes, as a function of composition, are also apparent in the spectra, which in addition provide information on the mixing behavior in both phases. We first discuss the *sn*-2 $^{13}C{=}O$ and ^2H head group spectra and then the ^2H chain spectra.

In Figure 11 we show the residual ^{13}C chemical shift anisotropy, $\overline{\Delta\sigma}$, as a function of composition at $T = 25$ °C and $T = T_{onset}$.[3] In all mixtures both DPPE and DPPC display almost the same shift anisotropy, and the $\overline{\Delta\sigma}$ of the mixture decreases with increasing DPPE content. This decrease is however not linear, as is indicated by the deviations from the straight line connecting the $\overline{\Delta\sigma}$ values for pure 2[1-^{13}C]DPPC and 2[1-^{13}C]DPPE. The fact that both components display approximately the same $\overline{\Delta\sigma}$ values in the gel state suggests that the orientation of the *sn*-2 $^{13}C{=}O$ tensor of both lipids in the mixture is similar. At the same time, the compositional

[3] The temperature where the characteristic L_α-like line or powder pattern starts to be visible was taken as T_{onset}. Likewise, the temperature where the gel-type spectrum had disappeared was defined as T_{comp}.

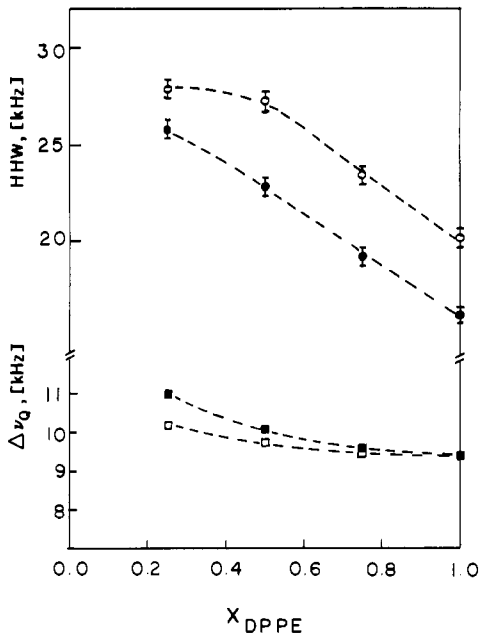

FIGURE 12: Half-height width (HHW) and residual quadrupole splitting $\Delta\nu_{Q\perp}$ of $^+NH_3$–CH_2–CD_2–DPPE in mixtures with DPPC: (○) HHW at 25 °C; (●) HHW at $T = T_{onset}$; (□) $\Delta\nu_{Q\perp}$ at 68 °C; (■) $\Delta\nu_{Q\perp}$ at $T = T_{comp}$.

dependence of $\overline{\Delta\sigma}$ depicted in Figure 11 indicates that a slight conformational changes take place in the backbone region to accommodate the other component.

A similar compositional dependence is observed in the ^2H spectra of head group labeled DPPE in the gel phase. In the top half of Figure 12 we show plots of the width of the gel-phase head group spectra of Figure 6 vs. X_{DPPE} at 25 °C and at T_{onset}. Above ~40% DPPE the width of the line decreases with increasing DPPE content of the mixture, indicating that the angular excursions of the head group become less restricted. Below ~40% DPPE the 25 °C curve appears to level off, suggesting no further changes in the average conformation of the head group at this temperature. We believe that the curves in both Figure 11 and Figure 12 can be understood on the basis of a gradual change in the gel-state lattice type exhibited by DPPC/DPPE mixtures.

It is well-known that DPPC at 25 °C is in the $L_{\beta'}$ phase, with the chains tilted at an angle of ~30° with respect to the bilayer normal (Tardieu et al., 1973; Janiak et al., 1976, 1979). The tilting of the chains overcomes the problem of cross sectional area mismatch between the large choline head group and the smaller acyl chains. In PE's, which possess a smaller head group, this problem does not occur, and the acyl chains are therefore oriented parallel to the bilayer normal in the L_β configuration (McIntosh, 1980). In a mixture it would be expected that the lattice type, $L_{\beta'}$ ($P_{\beta'}$) or L_β, would depend on the composition, and in fact, McIntosh (1980) has observed that incorporation of *n*-alkanes into DPPC bilayers can remove the tilt present in the pure system. The decrease in $\overline{\Delta\sigma}$ and in the width of the head group spectra observed with increasing PE content may therefore be due to a gradual transformation from an $L_{\beta'}$ to an L_β lattice. The data suggest this change is complete at 40–50% DPPE and is consistent with the temperature dependence of the spectra as a function of composition.

For example, we note that the shape of the $\overline{\Delta\sigma}$ vs. X_{DPPE} curves are nonlinear at low DPPE concentrations but become linear for $X_{DPPE} > 0.4$–0.5. Similarly, at 25 °C and at 40–50% DPPE, the width of the head group spectrum begins to decrease to the limiting value obtained for pure DPPE. Both of the effects suggest that introduction of PE into the PC lattice progressively relieves the packing constraints imposed by the choline head group. The result is a small conformational change at the *sn*-2 C=O, and the narrower head group spectrum indicates increased motional freedom in the part of the DPPE molecule.

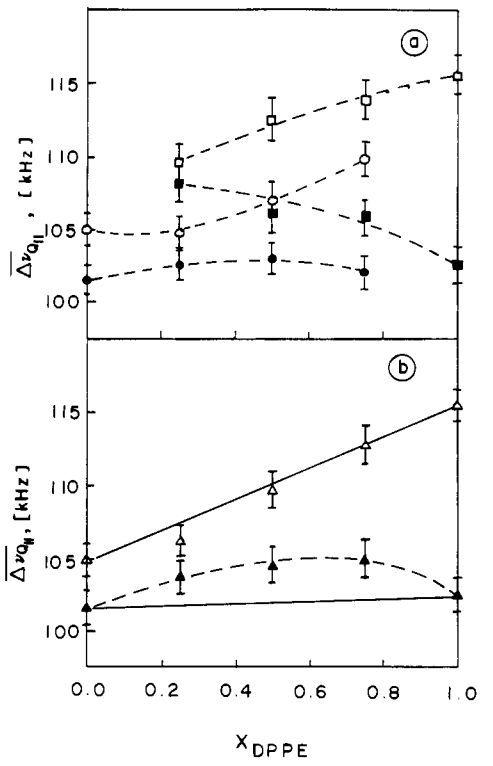

FIGURE 13: (a) Splitting of the parallel edges of the ^2H NMR powder patterns $\overline{\Delta\nu_{Q\parallel}}$ in DPPC/DPPE mixtures in the gel phase: (○) 2-[4,4-$^2H_2$]DPPC at 25 °C; (●) 2[4,4-$^2H_2$]DPPC at $T = T_{onset}$; (□) 2[4,4-$^2H_2$]DPPE at 25 °C; (■) 2[4,4-$^2H_2$]DPPE at $T = T_{onset}$. (b) Average splitting of the parallel edges of the ^2H NMR powder patterns $\Delta\nu_{Q\parallel}$ calculated as indicated in text from the data of Figure 13a: (△) at 25 °C; (▲) at $T = T_{onset}$.

In addition we have noted above that at these DPPE concentrations we begin to observe the simultaneous appearance of sharp liquid-crystalline components in both the ^{13}C and ^2H spectra. We have associated this phenomenon with the transformation of an L_β lattice to a two-phase region. In contrast at lower DPPE concentrations the appearance of the sharp component in the ^{13}C spectra precedes the appearance of a similar component in the ^2H spectra, indicating the presence of a $P_{\beta'}$ intermediate phase (see Figure 8). Thus, the data in Figures 12 and 13 are consistent with this interpretation. Finally, the deviation from linearity seen in Figure 11 may be an indication for nonideal mixing behavior in the gel phase as postulated previously, but on the basis of a simplified phase diagram (Mendelsohn & Koch, 1980). The data seem to exclude the possibility of monotectic behavior, since the $\Delta\sigma$ value of the pure compounds is not retained.

In principle the line shapes observed in the head group spectra can provide information on both the rate and mechanism of motional narrowing processes. For example, in glycolipids and in pure PE (Huang et al., 1980; Blume et al., 1982) we have employed computer simulations of ^2H spectra to study such processes. However, the head group in PE can assume a large number of conformations (Frischleder et al., 1981; Kovacs et al., 1980), and thus a description of the motion of the head group in the gel or liquid-crystalline state would contain numerous assumptions. For example, it would be

necessary to specify which conformations are preferred, as well as data on the rates of interconversion among these conformations. In addition, the internal motion would have to be superimposed on the long-axis diffusion. In view of these uncertainties we have not attempted to simulate the head group spectra in detail. Nevertheless, the width of the spectrum in the gel state is similar to that observed in the L_α phase and indicates that the motional processes that are responsible for the narrowing are probably similar in both phases. Moreover, since the spectral widths are about an order of magnitude smaller than the rigid lattice quadrupole couplings, the motion must be pseudo-isotropic. The presence of such motions will lead to substantial reductions in quadrupole echo intensities when the rates are in the range of 10^4 s^{-1}. Since such reductions in intensity are observed in the head group spectra, we can conclude that this is the order of magnitude of the exchange rates involved.

There are two additional points about the head group spectra worth noting. First, head group spectra as a function of composition show that for a particular temperature below the transition (e.g., 25 °C) the width of the ^2H spectrum increases with increasing PC content. The restrictions on the motional freedom of the PE head groups obviously depend on the PC content, and qualitatively this can be attributed to the larger size of the choline moiety. Second, a quantitative comparison of the echo intensities observed in 3:1, 1:1, and 1:3 mixtures at 1 °C shows that the reduction of the echo intensity is much larger for the 3:1 DPPC/DPPE mixture than for the mixtures with high DPPE content. This observation suggests slower motions in the head group region when large amounts of DPPC are present in the mixture.

In the liquid-crystalline phase well-resolved ^2H spectra are observed for the head group, and the residual quadrupole splittings, $\Delta\nu_{Q\perp}$, are plotted vs. X_{DPPE} in the lower half of Figure 12. From this figure it can be seen that an increase in the DPPE content results in smaller $\Delta\nu_{Q\perp}$ values at both the completion of melting and at 68 °C. Although the effects are not large, they do suggest that the presence of the larger choline head groups restricts the angular fluctuations of the ethanolamine moiety. Thus, the head group crowding effect due to the DPPC choline apparently influences the motional properties of the ethanolamine in qualitatively the same way in both the gel and liquid-crystalline phases.

Finally, the ^2H gel-phase and liquid-crystalline-phase spectra of chain-labeled DPPC/DPPE mixtures also exhibit some interesting and unexpected effects. Inspection of the spectra of Figures 3 and 4 shows that the gel-state spectra of both 2[4,4-$^2H_2$]DPPC and 2[4,4-$^2H_2$]DPPE in the lipid mixtures are qualitatively the same. Moreover, the line shapes are similar to those observed for pure DPPC and DPPE and may be simulated with axial diffusion rates of about 4×10^5 s^{-1} (Blume et al., 1982). The chains are not, however, in a strictly all-trans conformation as is illustrated in Figure 13a. Here we have plotted the separation between the parallel edges of the powder patterns vs. X_{DPPE} at 25 °C and T_{onset}. From these plots it can be discerned that the parallel edges are not separated by 125 kHz, as would be expected from all-trans conformation; instead, they are 10–20 kHz narrower. Furthermore, there are differences between the widths of the spectra exhibited by each component, and both are composition dependent, although not in the same way, at each temperature. It is also apparent that DPPC invariably exhibits a narrower spectrum than does DPPE at a given composition.

The reduced width is most easily explained by envoking a small amount of trans–gauche isomerization at the 4 position

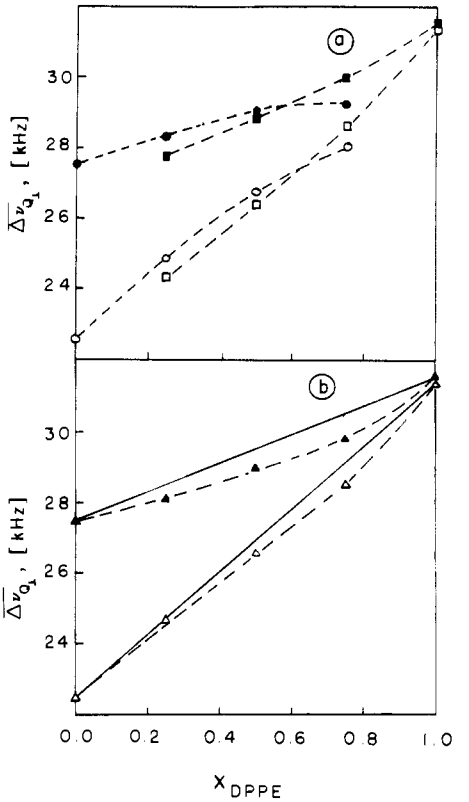

FIGURE 14: (a) Quadrupole splittings $\Delta\nu_{Q\perp}$ in the liquid-crystalline phase of DPPC/DPPE mixtures: (○) 2[4,4-$^2H_2$]DPPC at 68 °C; (●) 2[4,4-$^2H_2$]DPPC at $T = T_{comp}$; (□) 2[4,4-$^2H_2$]DPPE at 68 °C; (■) 2[4,4-$^2H_2$]DPPE at $T = T_{comp}$. (b) Average quadrupole splitting $\overline{\Delta\nu_{Q\perp}}$ calculated from the values in Figure 14a: (△) at 68 °C; (▲) at $T = T_{comp}$.

of each chain. In order to produce the required narrowing, it is necessary to reduce the trans population to about 0.90 and 0.95 for DPPC and DPPE, respectively. On a microscopic scale the fact that DPPC always exhibits a narrower spectrum than DPPE may be due again to head group crowding as was discussed above. Similar conclusions have been reached for solid DPPC and DPPE from IR and Raman investigations (Akutsu et al., 1981). Notice also that at 25 °C there is a change in the shape of these curves at DPPE $\simeq$ 0.4–0.5, and this is consistent with the $L_{\beta'}$ to L_β lattice transformation discussed above. At T_{onset} similar effects in the widths of the spectra are seen, but the composition dependence is noticeably different. This fact is better illustrated in Figure 13b, where we have plotted the average width of the spectra of the two components as a function of composition. The data for these curves were calculated from

$$\overline{\Delta\nu_{Q\parallel}} = X_{DPPC}\Delta\nu_{Q\parallel}(DPPC) + X_{DPPE}\Delta\nu_{Q\parallel}(DPPE) \quad (4)$$

where $\Delta\nu_{Q\parallel}$(DPPC) and $\Delta\nu_{Q\parallel}$(DPPE) are the splittings of the parallel edges of the powder patterns of pure DPPC and DPPE at the respective temperatures. At 25 °C a linear dependence of this quantity is observed, whereas at T_{onset} a clear positive deviation from linearity is observed. These curves will be discussed further below.

In the liquid-crystalline phase the spectra narrow dramatically and Figure 14a shows the composition dependence of $\Delta\nu_{Q\perp}$ for the two components at 68 °C and T_{comp}. As is clear from this figure, addition of DPPE to DPPC results in an increase in the quadrupole splitting, and at a given composition, both chains exhibit similar but not identical splittings. Qualitatively the same behavior is observed at T_{comp}, as can be seen in the figure. Finally, in Figure 14b are shown curves

for $\overline{\Delta\nu_{Q\perp}}$ calculated as above, but in this phase a negative deviation from ideality is apparent.

Together, these two figures suggest that addition of DPPE to DPPC, or vice versa, does not result in dramatic changes in either the structural or the dynamic properties of the acyl chains in either the gel or liquid-crystalline phase. Similar conclusions for the ^{13}C glycerol region of the lipids were obtained from the ^{13}C spectra. In view of the fact that the two lipids differ only in the N-terminal part of the head group, this result is not unexpected. At the same time, this question, the effect of PE on PC in these phases, has not heretofore been addressed on a microscopic scale, and thus this result is new. The small effects observed here are of course in marked contrast to those observed when cholesterol is the second liquid in the mixture (Haberkorn et al., 1978; Blumę & Griffin, 1982).

In previous discussions of the phase behavior of lipid mixtures (Lee, 1978; von Dreele, 1978; Freire & Snyder, 1980a,b; Cheng, 1980; Mendelsohn & Koch, 1980) the phase diagrams were analyzed on the assumption of regular solution theory. The conclusions of these studies was that binary mixtures of PC's, where the acyl chains differ by two or more methylene groups, as well as PC/PE mixtures show nonideal mixing behavior in both the gel and liquid-crystalline phases. Similarly, monolayer experiments on the related DMPC/DMPE system indicate a lattice condensation in the gel phase and an expansion in the liquid-crystalline phase (A. Blume, unpublished results). The NMR results in Figures 13b and 14b provide direct evidence for these effects. Namely, in the gel state a condensation effect is present, which is manifest in a slightly larger powder pattern breadths, whereas in the liquid phase the opposite effect is observed due to a lattice expansion. NMR thus provides a direct and facile means to detect those nonidealities. In particular, eq 4 requires that the average splitting should change in a linear fashion in a system with ideal mixing, and thus any observed deviation from linearity must indicate nonideal mixing. Physically this requires that on the time scale of the NMR experiment, the lateral diffusion or exchange in the mixture must be fast compared to the difference in the quadrupole splittings of the two components. Finally, one might speculate as to whether or not the higher transition enthalpies observed for a 1:1 mixture of DPPC/DPPE (Blume, 1980), and for other binary PC mixtures (Mabrey & Sturtevant, 1976) or PC/PE mixtures (Blume & Ackermann, 1974), are related to the deviations from ideality seen in the NMR experiments. Qualitatively the results go in the right direction in that the gel phase is condensed and the liquid-crystalline phase expanded; therefore, a larger change in internal energy would be expected at the phase transition. However, in the particular case of DPPC/DPPE the effects are relatively subtle, so that it would be better to examine a system where the nonideality is more pronounced, for instance DMPE/DSPC (Blume & Ackermann, 1974; Lee, 1978).

Conclusions. In the last decade phase equilibria in multiple-component lipid mixtures have been investigated extensively. However, with few exceptions these studies have relied on extrinsic probes such as spin or fluorescence labels or on macroscopic measurements like DSC to determine the position of phase boundaries. As a consequence, the microscopic properties of the systems, i.e., molecular conformations and dynamics, and the way in which the properties vary with temperature and composition have remained uncertain. The results presented here are a first attempt to rectify this situation and have yielded a number of interesting results for the gel and liquid-crystalline phases and for the two-phase region of DPPC/DPPE mixtures.

Because both the ^{13}C and ^{2}H NMR spectra change precipitously at phase boundaries, they permit the accurate location of the boundaries without the complication produced by an external probe. Concurrently, the motional averaging processes, which lead to these spectral effects, can be related to changes in the molecular conformation of the lipids, as well as to the rates of the associated dynamic processes. Thus, the melting of the acyl chains is apparent in the ^{2}H spectra, and the conformation change in the glycerol backbone can be deduced from the ^{13}C results. Furthermore, the superposition of spectra observed in the two-phase region of the phase diagram indicates that the rates of exchange between the solid and liquid domains are slow and that the domain size is large. The behavior of the DPPC/DPPE system also makes it clear that the phase transition mechanism in a mixed lipid system can be a function of the composition. In this particular case the change in the transition mechanism results from the gel state transforming from an $L_{\beta'}$ or $P_{\beta'}$ to an L_{β} lattice with increasing DPPE concentration. This observation also emphasizes the importance of performing multiple measurements in this sort of investigation.

The type of experiments described here should prove useful in investigations of other lipid mixtures. For instance, analysis of lipid mixtures where gel-state immiscibility is known to occur, and liquid immiscibility is postulated, should prove amenable to investigation. Specific labeling could also provide insight into the preferential interaction of nonlipid molecules—e.g., anesthetics or proteins—with one or more members of a multicomponent lipid mixture, a situation that may occur in biological membranes.

References

Akutsu, H., Ikematsu, M., & Kyogoku, Y. (1981) *Chem. Phys. Lipids 28*, 149.

Arnold, K., Lösche, A., & Gawrisch, K. (1981) *Biochim. Biophys. Acta 645*, 143.

Blume, A. (1976) Ph.D. Thesis, University of Freiburg, West Germany.

Blume, A. (1980) *Biochemistry 19*, 4908.

Blume, A., & Ackermann, T. (1974) *FEBS Lett. 43*, 71.

Blume, A., & Griffin, R. G. (1982) *Biochemistry* (second paper of three in this issue).

Blume, A., Rice, D. M., Wittebort, R. J., & Griffin, R. G. (1982) *Biochemistry* (first paper of three in this issue).

Chakrabarti, P., & Khorana, H. G. (1975) *Biochemistry 14*, 5021.

Chapman, D., Urbina, J., & Keough, K. M. (1974) *J. Biol. Chem. 249*, 2512.

Cheng, W. H. (1980) *Biochim. Biophys. Acta 600*, 358.

Das Gupta, S. K., Rice, D. M., & Griffin, R. G. (1982) *J. Lipid Res. 23*, 197.

Davis, J. H., Jeffrey, K. R., Bloom, M., Valic, M. I., & Higgs, T. P. (1976) *Chem. Phys. Lett. 42*, 390.

Devaux, P., & McConnell, H. M. (1972) *J. Am. Chem. Soc. 94*, 4477.

Eibl, H. (1978) *Proc. Natl. Acad. Sci. U.S.A. 75*, 4074.

Freire, E., & Snyder, B. (1980a) *Biochemistry 19*, 88.

Freire, E., & Snyder, B. (1980b) *Biochim. Biophys. Acta 600*, 643.

Frischleder, H., Krahl, R., & Lehmann, E. (1981) *Chem. Phys. Lipids 28*, 291.

Galla, H. J., Hartmann, W., Theilen, V., & Sackmann, E. (1979) *J. Membr. Biol. 48*, 215.

Griffin, R. G. (1981) *Methods Enzymol. 72*, 108.

Gupta, C. M., Radakrishnan, R., & Khorana, H. G. (1977) *Proc. Natl. Acad. Sci. U.S.A. 74*, 4315.
Haberkorn, R. A., Griffin, R. G., Meadows, M. D., & Oldfield, E. (1977) *J. Am. Chem. Soc. 99*, 7353.
Huang, T-H., Skarjune, R. P., Wittebort, R. J., Griffin, R. G., & Oldfield, E. (1980) *J. Am. Chem. Soc. 102*, 7377.
Hui, S. W. (1981) *Biophys. J. 34*, 383.
Janiak, M. J., Small, D. M., & Shipley, G. G. (1976) *Biochemistry 15*, 4575.
Janiak, M. J., Small, D. M., & Shipley, G. G. (1979) *J. Biol. Chem. 254*, 6068.
Kovacs, A. L., Brosio, E., Conti, F., DiNola, A., & Napolitano, G. (1980) *Chem. Phys. Lipids 27*, 113.
Lee, A. G. (1976) *Biochemistry 15*, 2448.
Lee, A. G. (1978) *Biochim. Biophys. Acta 507*, 433.
Lentz, B. R., Freire, E., & Biltonen, R. L. (1978) *Biochemistry 17*, 4475.
Luna, E. J., & McConnell, H. M. (1977) *Biochim. Biophys. Acta 470*, 303.
Luna, E. J., & McConnell, H. M. (1978) *Biochim. Biophys. Acta 509*, 462.
Mabrey, S., & Sturtevant, J. M. (1976) *Proc. Natl. Acad. Sci. U.S.A. 73*, 3862.
McIntosh, T. J. (1980) *Biophys. J. 29*, 237.
Mendelsohn, R., & Taraschi, T. (1978) *Biochemistry 17*, 3944.
Mendelsohn, R., & Koch, C. C. (1980) *Biochim. Biophys. Acta 598*, 260.
Naqvi, K. R., Behr, J. P., & Chapman, D. (1974) *Chem. Phys. Lett. 26*, 440.
Pines, A., Gibby, M. G., & Waugh, J. S. (1973) *J. Chem. Phys. 59*, 569.
Rouser, G., Nelson, G. J., Fleischer, S., & Simon, G. (1968) in *Biological Membranes* (Chapman, D., Ed.) pp 5–69, Academic Press, London.
Rubinstein, J. L. R., Smith, B. A., & McConnell, H. M. (1979) *Proc. Natl. Acad. Sci. U.S.A. 76*, 15.
Sackmann, E., & Träuble, H. (1972) *J. Am. Chem. Soc. 94*, 4482.
Seelig, J., & Gally, H. (1976) *Biochemistry 15*, 1599.
Shimshick, E. J., & McConnell, H. M. (1973) *Biochemistry 12*, 2351.
Sklar, L. A., Hudson, B., & Simoni, R. P. (1977) *Biochemistry 16*, 819.
Solomon, I. (1958) *Phys. Rev. 110*, 61.
Spiess, H. W., & Sillescu, H. (1981) *J. Magn. Reson. 42*, 381.
Stamatoff, J., Feuer, B., Guggenheim, H., Tellez, G., & Yamane, T. (1982) *Biophys. J. 38*, 217.
Tardieu, A., Luzzati, V., & Reman, F. C. (1973) *J. Mol. Biol. 75*, 711.
von Dreele, P. H. (1978) *Biochemistry 17*, 3939.
Weissbach, H., & Sprinson, D. B. (1953) *J. Biol. Chem. 203*, 1031.
Wittebort, R. J., Schmidt, C. F., & Griffin, R. G. (1981) *Biochemistry 20*, 4223.
Wittebort, R. J., Blume, A., Huang, T-H., Das Gupta, S. K., & Griffin, R. G. (1982) *Biochemistry 21*, 3487.
Wu, E. S., Jacobson, K., & Papahadjopoulos, D. (1977) *Biochemistry 16*, 3936.

High-Resolution Proton Nuclear Magnetic Resonance Studies of the Nickel(II) Derivative of Azurin†

Judith A. Blaszak, Eldon L. Ulrich, John L. Markley, and David R. McMillin*

ABSTRACT: High-resolution (360 and 470 MHz) ^{1}H NMR studies of Ni(II) azurin, the nickel(II) derivative of the blue copper protein azurin, are reported. The aliphatic resonances of Ni(II) azurin closely parallel those of apoazurin and Cu(I) azurin and indicate that no major structural changes are associated with the binding of nickel(II). The magnetic moment of Ni(II) azurin (μ_{eff} = 3.2 μ_B) is in keeping with a pseudotetrahedral coordination environment like that of Cu(I) azurin. Resonances of protons from the ligand moieties are shifted as far as 125 ppm downfield from 4,4-dimethyl-4-silapentane-1-sulfonate and as far as 20 ppm upfield by internal fields due to the nickel center. One of these strongly shifted resonances is assigned to the methyl protons of the methionine ligand. From spectra of Ni(II) azurin as a function of pH, the pK_a' values of histidine-35 and histidine-83 have been measured to be ~6.0 and 7.5, respectively. Histidine-35 titrates in a discontinuous fashion, and, significantly, so do several of the isotropically shifted ligand protons, also within experimental error with the same pH_{mid}. This result reinforces the suggestion that the conformational change coupled to the protonation of histidine-35 plays an important role in regulating electron transfer reactions of native azurin [Silvestrini, M. C., Brunori, M., Wilson, M. T., & Darley-Usmar, V. M. (1981) *J. Inorg. Biochem. 14*, 327–338].

Azurin is a soluble, type I, blue copper protein. The azurin from anaerobically cultured *Pseudomonas aeruginosa* has been purified to homogeneity (Ambler & Brown, 1967), and its primary sequence has been determined (Ambler, 1971). Azurin has been studied extensively by a variety of physical methods (Fee, 1975; Gray & Solomon, 1981), including electronic spectroscopy (Brill et al., 1968; McMillin et al., 1974; Solomon et al., 1976, 1980; McMillin, 1978; Tennent & McMillin, 1979; McMillin & Morris, 1981), NMR spectroscopy (Hill & Smith, 1976, 1978, 1979; Hill et al., 1976; Ugurbil & Bersohn, 1973; Ugurbil et al., 1977), and X-ray crystallography (Adman et al., 1978; Adman & Jensen, 1981); these studies have examined the nature and disposition of the copper ligands as well as the protein fold. Various roles have been envisaged for the protein structure, including (i) con-

† From the Department of Chemistry, Purdue University, West Lafayette, Indiana 47907. *Received June 8, 1982.* J.A.B. and D.R.M. were supported by National Institutes of Health Grant GM 22764. E.L.U. and J.L.M. were supported by the Competitive Research Grants Office, the Cooperative State Research Service, the Science and Education Administration, the U.S. Department of Agriculture, and National Institutes of Health Grant RR01077.

0006-2960/82/0421-6253$01.25/0